Dehydration Induces Lateral Expansion of Polyunsaturated 18:0–22:6 Phosphatidylcholine in a New Lamellar Phase

H. Binder* and K. Gawrisch†

*University of Leipzig, Institute of Medical Physics and Biophysics, D-04103 Leipzig, Germany; †National Institutes of Health, National Institute on Alcohol Abuse and Alcoholism, Laboratory of Membrane Biochemistry and Biophysics, Rockville, Maryland 20852 USA

ABSTRACT To gain a better understanding of the biological role of polyunsaturated phospholipids, infrared (IR) linear dichroism, NMR, and x-ray diffraction studies have been conducted on the lyotropic phase behavior and bilayer dimensions of *sn*-1 chain perdeuterated 1-stearoyl-2-docosahexaenoyl-*sn*-glycero-3-phosphocholine (SDPC-d35), a mixed-chain saturated (18:0)-polyunsaturated (22:6ω3) lipid. SDPC films were hydrated at definite values of temperature (T) and relative humidity (RH). In excess water, the lipid forms exclusively lamellar phases in the temperature range 0–50°C. Upon dehydration the lipid undergoes the main phase transition between the liquid-crystalline (L_α) and gel (L_β) phase at $T < 15$°C. Both the saturated and polyunsaturated chains adopt a stretched conformation in the L_β phase, presumably the all-*trans* (stearoyl) and angle iron or helical (docosahexaenoyl) one. A new fluid lamellar phase (L_α') was found in partially hydrated samples at $T > 15$°C. SDPC membranes expand laterally and contract vertically in the L_α' phase when water was removed. This tendency is in sharp contrast to typical dehydration-induced changes of membrane dimensions. The slope of the phase transition lines in the RH-T phase diagram reveal that the lyotropic L_α'-L_α and L_β-L_α transitions are driven by enthalpy and entropy, respectively The possible molecular origin of the phase transitions is discussed. The properties of SDPC are compared with that of membranes of monounsaturated 1-palmitoyl-2-oleoyl-*sn*-glycero-3-phosphocholine (POPC-d31).

INTRODUCTION

Phospholipids, with saturated acyl chains in the *sn*-1 and unsaturated acyl chains in the *sn*-2 glycerol backbone position, represent the most abundant membrane lipid class (White, 1973). Physico-chemical studies have largely dealt with lipids composed of either symmetric saturated chains or those with *sn*-2 chains containing only a single double bond. Polyunsaturated lipids with multiple double bonds in the *sn*-2 chain, however, constitute a considerable fraction of lipids in neuronal tissues and the retina. Particularly, near-native levels of 50% of docosahexaenoyl (DHA, 22:6ω3) chains in retinal rod outer segment disk membranes are required for proper function of the visual receptor rhodopsin (see Mitchell et al., 1998, and references therein). The content of DHA in gray brain tissue is consistently 20–30% in 45 animal species (Crawford et al., 1977). The fact that DHA accumulates at high concentration in neural membranes raises the possibility that it may alter membrane biophysical properties important for function.

There exists an extensive literature concerned with the importance of DHA for human health, but comparatively little research has been done on the physical properties of this important molecule. Early theoretical (Albrand et al., 1994; Applegate and Glomset, 1986) and spectroscopic (Litman et al., 1991; Paddy et al., 1985; Salmon et al., 1987) studies deal with conformational and packing properties of polyunsaturated chains in membranes. Investigations were considerably intensified over the last few years to find out how such oxidation-prone, exotic lipids affect membrane molecular architecture and dynamics (Everts and Davis, 2000; Holte et al., 1995; Separovic and Gawrisch, 1996) as well as mechanical properties such as lateral compressibility (Huster et al., 1999; Koenig et al., 1997; Rawicz et al., 2000) and water permeability (Huster et al., 1997; Olbrich et al., 2000).

An essential outcome of these studies has been that polyunsaturation loosens chain packing and decreases the strength of cohesive interactions in the membranes. As a consequence, bending stiffness is decreased (Rawicz et al., 2000) and water permeability increased in comparison with membranes of saturated and monounsaturated lipids (Huster et al., 1997; Olbrich et al., 2000). Moreover, it was proposed that polyunsaturated chains, when paired with saturated ones, cause subtle changes of membrane lateral organization and interfacial properties, which may provide the key to understanding the effect of multiple *cis* double bonds in lipid acyl chains (Holte et al., 1995). It was observed that chain order parameters of saturated chains are lower when paired with polyunsaturated DHA. In particular, order of the segments from the second half to the chains near the bilayer center was lower, perhaps, indicating an altered profile of lateral tension across the bilayer. Polyunsaturation results in a thinner bilayer and an increased area per lipid in almost fully hydrated membranes (Koenig et al., 1997).

Hydration studies on lipids not only provide information on water-binding properties but also probe elastic properties of lipid aggregates (Binder et al., 1999b; Koenig et al., 1997; Parsegian et al., 1979) and lipid phase behavior (Binder et al., 1997, 1999a). Phase transitions between

Received for publication 12 October 2000 and in final form 23 April 2001.

Address reprint requests to Dr. Hans Binder, University of Leipzig, Institute of Medical Physics and Biophysics, Liebigstrasse 27, D-04103 Leipzig, Germany. Tel.: 49-341-2326160; Fax: 49-341-9715709; E-mail: binder@rz.uni-leipzig.de.

0006-3495/01/08/969/14 $2.00

lamellar and nonlamellar, solid gel or subgel, and liquid-crystalline phases reveal microscopic characteristics such as preferred shape, flexibility/rigidity, and hygroscopicity of the molecules and the intermolecular forces acting between them on a macroscopic level.

The degree of hydration of amphipathic structures is thermodynamically determined by the chemical potential of water in the system. In combination with temperature, the chemical potential of water represents an independent thermodynamic degree of freedom, and its variation opens up novel opportunities to study physico-chemical properties of lipids. The degree of hydration of lipid films can be easily varied by exposing the sample to an atmosphere of definite relative humidity (RH). Recently we used this method to study the effect of conjugated double bonds in lipid acyl chains on phase behavior and membrane architecture of diene lipids (Binder et al., 1997, 1999a,c, 1998; Binder and Kohlstrunk, 1999). The main purpose of the present investigation was to obtain the RH-T phase diagram of SDPC and to determine the mean dimensions of lipid bilayers as a function of hydration. We combined infrared (IR) linear dichroism, x-ray, and NMR techniques that are well suited to study lipid phases in terms of aggregate morphology, local interactions, and molecular ordering. The monounsaturated 1-palmitoyl-2-oleoyl-*sn*-glycero-3-phosphocholine (POPC) was included in the study for the sake of comparison between poly- and monounsaturated lipids. Perdeuterated lipid analogs were used to obtain specific signals of the acyl chains in *sn*-1 and *sn*-2 positions.

The most interesting observation of this study has been the detection of a novel liquid-crystalline lamellar phase of SDPC that expands laterally upon dehydration. This unusual behavior contradicts typical phase diagrams of membranes of disaturated and monounsaturated lipids. A hypothesis that may explain this surprising tendency is presented.

MATERIALS AND METHODS

Materials

The lipids SDPC and POPC and their perdeuterated analogs (SDPC-d35 and POPC-d31) were purchased from Avanti Polar Lipids (Alabaster, AL). The stearic acid chain is ~98% deuterated (Holte et al., 1995), except for the C_2 methylene segment that is deuterated to ~50% only. To minimize oxidation of SDPC and SDPC-d35, the lipids were stored as methylene chloride stock solutions with butylated hydroxy toluene (BHT) added at a molar lipid-to-BHT ratio of 250:1. Lipid purity was checked by matrix-assisted laser desorption and ionization time-of-flight mass spectrometry (MALDI-TOF-MS), which detects lipid peroxidation products with high sensitivity. Concentration of peroxidation products in freshly prepared samples was lower than the detection limit, corresponding to lipid purity of better than 98% (Schiller et al., 1998). Lipid samples were studied by infrared spectroscopy over a period of up to 2 weeks after preparation. Initially sharp lyotropic phase transitions become broad after a few days of storage in the sample cell of the spectrometer owing to degradation of the lipid. We used the sharpness of the gel-to-liquid crystalline phase transition of freshly prepared SDPC and SDPC-d35 as a criterion of the integrity of the lipid (see below). The sharpness of the phase transition was tested after each series of Fourier transform infrared (FTIR) measurements. X-ray measurements were performed within 1 day after preparation.

Infrared measurements

Appropriate amounts of the stock solution were spread on the surface of a ZnSe-attenuated total reflection (ATR) crystal for sample preparation (angle of incidence, 45°; six active reflections). The solvent evaporates under a stream of nitrogen within a time of less than 1 min. The amount of material corresponds to an average thickness of the lipid films of >3 μm, or equivalently, to a stack of >500 bilayers in the lamellar phase. Consequently, the films represent bulk samples despite their macroscopic orientation on the surface of the ATR crystal (vide infra). The ATR crystal was immediately mounted inside a sample chamber that protects the lipid film from visible light and from aerobic conditions (Binder et al., 1997). The sample chamber was placed into a BioRad FTS-60a FTIR spectrometer (Bio-Rad, Cambridge, MA) equipped with a wire grid polarizer. Polarized absorption spectra, $A_{\parallel}(\nu)$ and $A_{\perp}(\nu)$, were recorded with light polarized parallel and perpendicular with respect to the plane of incidence (128 accumulations each). Band positions were analyzed by means of their center of gravity (COG) in the weighted sum spectrum, $A(\nu) = A_{\parallel}(\nu) + 2.55\, A_{\perp}(\nu)$ (Binder and Schmiedel, 1999).

The lipid films were hydrated by blowing a definite RH, high-purity nitrogen gas through the sample chamber. The temperature (T) and RH were adjusted by means of a flowing water thermostat (Julabo, Seelbach, Germany) and a moisture generator (HumiVar, Leipzig, Germany) with an accuracy of ± 0.05 K and $\pm 0.5\%$ RH, respectively. The RH was increased in steps of ΔRH = 3% from 5% to 98% (hydration scan) or decreased in the opposite direction (dehydration scan) at constant T. The sample was allowed to equilibrate for 10 min before measurement at a given RH. No significant hysteresis effects between hydration and dehydration scans were detected, confirming that lipid hydration reached equilibrium. The hydration studies were also conducted as a function of RH of D_2O to improve the spectral analysis in the C=O stretching region, which overlaps with the H_2O bending band.

Determination of infrared order parameters

The IR order parameter of an absorption band, $S_{IR} \equiv \langle P_2(\theta_\mu)\rangle$, is defined as the second-order Legendre polynomial, $P_2(\theta_\mu) \equiv 0.5(3\cos^2\theta_\mu - 1)$, of the angle θ_μ between the respective transition moment, μ, and the ATR normal, n. The angular brackets denote spectroscopic averaging over all groups in the sample that absorb in the respective frequency range where the contribution of each group to the mean value is weighted by its integral absorption coefficient. The IR order parameter was calculated from the dichroic ratio of the integral, baseline-corrected polarized absorbances, $R = A_{\parallel}/A_{\perp}$ using Harrick's thick-film approximation (Harrick, 1967; see also Binder and Schmiedel, 1999, for details):

$$S_{IR} = (R - 2)/(R + 2.55) \quad (1)$$

Selective deuteration of the saturated acyl chains of the lipids allows evaluation of the molecular ordering of the stearoyl (SDPC-d35) and palmitoyl (POPC-d31) chains using the IR order parameters of the symmetric and antisymmetric CD_2 stretching bands near 2090 cm^{-1} and 2195 cm^{-1}, $S_{IR}(\nu_s(CD_2))$ and $S_{IR}(\nu_{as}(CD_2))$, respectively. Their transition moments are assumed to point perpendicular one to another and perpendicular to the fiber axis of the polymethylene chain. Consequently, both parameters can be combined to yield the apparent longitudinal order parameter of the deuterated acyl chains according to (Binder and Schmiedel, 1999)

$$S_\theta(\text{stearoyl, palmitoyl}) = -(S_{IR}(\nu_s(CD_2)) + S_{IR}(\nu_{as}(CD_2))), \quad (2)$$

which provides a measure of the mean orientation of the chain axis with respect to the ATR normal according to $S_\theta \equiv \langle P_2(\theta_z)\rangle$. The angle θ_z is enclosed between n and the interconnecting line between the midpoints of two successive C-C bonds. The longitudinal chain order parameter depends to a high degree on the conformational order of the methylene segments as indicated by a marked drop of S_θ at the chain melting transition of the lipids (see below). Additional effects such as tumbling motions of whole chains, imperfect alignment of the membranes on the ATR surface, fluctuations of the local director due to undulations of the bilayers, a permanent tilt of the chain axes, and also vibrational coupling along the chains can interfere with conformational ordering in lamellar phases. Moreover, bend monolayers in nonlamellar phases decrease IR order parameters considerably (Binder et al., 1999a; Binder and Pohle, 2000). All these effects can be considered in terms of a set of nested uniaxial order parameters if they act independently of each other:

$$S_\theta = \prod_i S_i, \quad \text{with} \quad S_i \equiv \langle P_2(\theta_i)\rangle \tag{3}$$

The indices $i = m, d, n$ refer to the angles between a set of axes, the ith of which distributes in a symmetrical fashion about axis $i + 1$. For example, θ_m is the angle between the chain axis m and the local director d whereas θ_d defines the angles between d and the ATR normal n.

The mean ordering of the proteated unsaturated chains of POPC-d31 and SDPC-d35 is also accessible in the IR linear dichroism experiment. The longitudinal order parameter of the polymethylene fragments of the oleoyl chains were determined from the IR order parameters of the symmetric and antisymmetric CH_2 stretches near 2852 cm^{-1} and 2922 cm^{-1}, respectively:

$$S_\theta(\text{oleoyl}) \equiv -(S_{IR}(\nu_s(CH_2)) + S_{IR}(\nu_{as}(CH_2))) \tag{4}$$

The IR order parameter of the C-H bending mode of the vinyl groups of the dososahexanoyl chains near 1388 cm^{-1} yields the longitudinal order parameter of the polyunsaturated chain:

$$S_\theta(\text{DHA}) \equiv S_{IR}(\delta(CH)) \tag{5}$$

This choice was motivated by the fact that $S_{IR}(\delta(\text{C-H}))$ nearly reaches its maximum possible value of unity in the L_β phase of SDPC-d35 (vide infra). Consequently, the corresponding transition moments must point along the chain axis for symmetry reasons. A detailed discussion of the linear dichroism of SDPC will be given elsewhere.

Gravimetric measurements

The stock solution was spread on the surface of a circular quartz slide (diameter 15 mm) and allowed to dry under a stream of nitrogen. The sample was placed into a twin microbalance system (Sartorius, Göttingen, Germany) that has been equipped with a moisture-regulating device (see above and Binder et al., 1997). The RH was adjusted by flowing moist, high-purity N_2 gas through the sample chamber. Before starting the experiments, the lipid was dried for 12–24 h at RH = 0% until the mass of the sample attained some constant value (~0.5 mg). The mass increment due to the adsorption of water was recorded in the continuous mode by scanning RH at a constant rate of $<\pm 10\%$ RH per hour covering the range of 0–98% RH. The mass increment yields the sorption isotherms presented as the molar water-to-lipid ratio, $R_{W/L}$.

X-ray measurements

For x-ray investigations, oriented multibilayer stacks of the lipids were prepared by spreading appropriate amounts of the stock solution on glass slides (20 × 25 mm). Subsequently, the organic solvent was evaporated. The slides were positioned into a sealed thermostatted (±0.5 K) chamber mounted at a conventional Philips PW3020 powder diffractometer (Philips, Eindhoven, The Netherlands). X-ray diffractograms were obtained with Ni-filtered Cu K_α radiation (20 mA/30 kV) by $\Theta_{x\text{-ray}}/2\ \Theta_{x\text{-ray}}$ scans monitoring the s-range s = 0.1–1.1 nm^{-1} ($s = 2\sin\theta/\lambda$, λ = 0.154 nm). The intensity was detected with a proportional detector system. Nitrogen of definite RH was continuously streamed through the sample chamber using a moisture-regulating unit (see above). The samples were investigated at discrete RH values and equilibrated for at least 1 h before measurements. Repeat distances of the lamellar phase, $d = ns^{-1}$ (n is an integer), were determined with an accuracy of ±0.1 nm using the Bragg peaks of up to fourth order (n = 1–4). The mean area requirement per lipid in the membrane plane was calculated by means of

$$A_L = 2(v_L + R_{W/L}v_w)/d, \tag{6}$$

where v_L and v_W denote the molecular volumes of lipid and water, respectively.

The mean thickness of the water gaps in the multibilayer stacks was estimated assuming nonpenetrating water and lipid layers (Luzzati, 1968):

$$d_w = 2R_{W/L}v_w/A_L \tag{7}$$

The thickness of the hydrophobic core of the bilayer was estimated by $d_{hc} = d_L - d_{pol}$, where $d_L = d - d_W$ denotes the thickness of the bilayer and $d_{pol} = 2v_{pol}/A_L$ is the thickness of the polar part of the bilayer. v_{pol} is the volume of the nonhydrated polar part of the lipids, which includes the glycerol and carbonyl moieties. We used a value of v_{pol} = 0.325 nm^3 (see (Nagle and Tristam-Nagle, 2000, and references therein). Consequently, the thickness of the hydrophobic core of one-half of the bilayer is $L_{hc} = 0.5d_{hc}$.

NMR experiments

NMR samples were prepared by removing the solvent under a stream of argon with subsequent brief application of vacuum. SDPC in excess water was prepared by adding 50 wt % of deuterium-depleted water. The lipid was transferred to a 4-mm glass sample tube that was sealed with a ground glass joint and cap. An SDPC sample at reduced water content was prepared by blowing argon gas with RH of 33% over a thin layer of dried lipid in a glass vial. The RH was adjusted by blowing the argon through a saturated salt solution of $MgCl_2$ that was thermostatted at 30°C. The hydrated lipid was collected at the bottom of the tube by centrifugation at 50,000 × g. The sample was sealed with a ground glass joint and cap as above. All preparation procedures were conducted in a glove box (Plas-Labs, Lansing, MI) that was filled with a 90% nitrogen/10% hydrogen gas mixture. Oxygen content was reduced to nondetectable levels by catalytically burning hydrogen. The resulting water vapor was adsorbed in a column. Samples were immediately investigated after preparation. Lipid integrity was verified by hydrolyzing small quantities of the sample and transmethylating the fatty acids. The ratio of saturated to polyunsaturated fatty acids was checked by gas chromatography. Any loss of DHA was less than the resolution of GC peak intensities (±1%).

The ^{31}P and ^2H NMR spectra were acquired on a Bruker DMX300 spectrometer using a high-power probe with a 4-mm solenoid sample coil tunable to both ^{31}P and ^2H resonance frequencies. Proton-decoupled ^{31}P NMR spectra at a resonance frequency of 121.4 MHz were collected with a Hahn echo sequence with a 1.8-s 90° pulse, a between-pulse delay of 50 μs, and a repetition rate of one acquisition per second. The spectral width was 125 kHz. Proton-noise decoupling resulted in sample heating of less than 1°C. The ^2H NMR spectra were acquired at a resonance frequency of 46.0 MHz using a quadrupolar echo pulse sequence with a 2.2-μs 90° pulse, a 50-μs delay between pulses, and a repetition rate of two acquisitions per second. De-Paked spectra (Sternin et al., 1983) were calculated using the algorithm of McCabe and Wassall (1995). Smoothed order

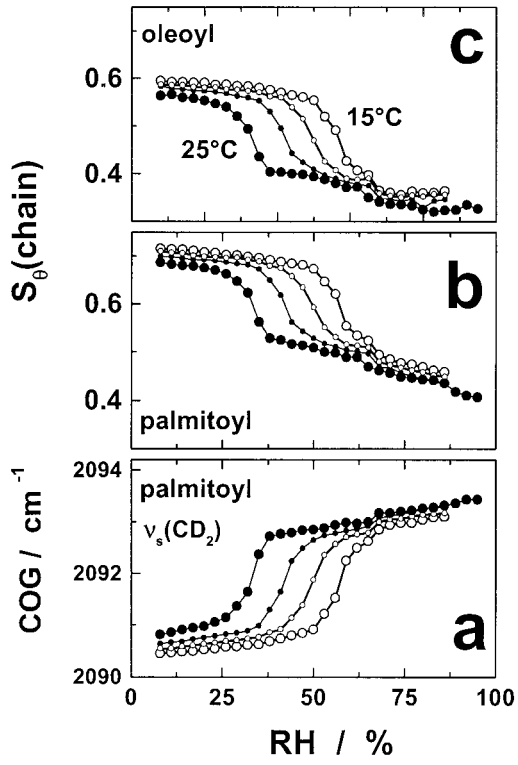

FIGURE 1 Center of gravity of the symmetric CD_2 stretching band (*a*) and longitudinal IR order parameter (S_θ) (*b*) of the deuterated palmitoyl chains of POPC-d31 as a function of RH. The temperature of the hydration scans was increased from T = 15°C (○) to 25°C (●) in steps of 3 K. (*c*) Longitudinal IR order parameter of the proteated oleoyl chain in the *sn*-2 position of POPC-d31.

parameter profiles of the stearic acid chain were computed according to the method of Lafleur et al. (1989).

RESULTS

Lyotropic gel/liquid-crystalline phase transition of POPC

For comparison with SDPC-d35, we first studied the lyotropic phase behavior and molecular order of monounsaturated POPC-d31. The choice of POPC-d31 is motivated by the similar main transition temperatures of fully hydrated SDPC ($T_m = -3.8 \pm 1.8$°C) and POPC ($T_m = -2.5 \pm 2.4$°C) (see (Koynova and Caffrey, 1998, and references therein) that enables comparison of phase behavior without introducing a reduced temperature scale.

Fig. 1 *a* depicts the center of gravity of the symmetric methylene stretching band of the deuterated palmitoyl chain (COG($\nu_s(CD_2)$)) as a function of RH at different temperatures. The graphs show the characteristics of a lyotropic chain melting transition between the lamellar gel (L_β) and liquid crystalline (L_α) phase. This event is characterized by a sigmoidal increase of COG by 1–3 cm^{-1}. RH scans at increased temperatures shift the RH of the phase transition to smaller RH values.

Fig. 1, *b* and *c*, depicts the longitudinal order parameter, S_θ, of the acyl chains of POPC-d31. It was calculated from the IR order parameters of the antisymmetric and symmetric methylene stretching bands of the deuterated palmitoyl and the proteated oleoyl chain by means of Eqs. 2 and 4, respectively. Also, the RH dependence of S_θ reveals chain melting by a distinct decrease in the intermediate RH range (Fig. 1). The significantly smaller values of S_θ(oleoyl) suggest reduced conformational order of the monounsaturated chain due to two effects: 1) the bent conformation that acyl chains typically adopt in the *sn*-2 position of 1,2-diacylglycero-lipids near the C2 atom and 2) the disordering effect of the *cis* double bond.

We found equal linear dichroism of antisymmetric and symmetric methylene stretching modes at all conditions (i.e., $S_{IR}(\nu_{as}(CD_2)) \approx S_{IR}(\nu_s(CD_2))$ for the palmitoyl chains within the error limits ($|\delta S_{IR}| < 0.03$). This result indicates cylindrical symmetry caused by rotations about the chain axis and/or the absence of a uniform tilt of the extended chains in contrast to the arrangement of the palmitoyl chains in the $L_{\beta'}$ phase of dipalmitoylphosphatidylcholine (DPPC) (Binder, 1999). Probably, the monounsaturated oleoyl chains prevent transverse ordering and/or tilting of the chains in the L_β phase of POPC.

IR evidence of lyotropic phase transitions of SDPC

The graphs of the center of gravity of the symmetric methylene stretching band of the deuterated stearoyl chain of SDPC-d35 (COG($\nu_s(CD_2)$)) as a function of RH show the characteristics of a lyotropic gel (L_β)-to-liquid-crystalline (L_α) chain melting transition at temperatures T ≤ 15°C (Fig. 2 *a*). The positive values of the longitudinal IR order parameter S_θ(stearoyl) > 0.3 indicate that the lipid membranes preferentially align parallel with the ATR surface (Fig. 2 *b*). The relation $S_{IR}(\nu_{as}(CD_2)) \approx S_{IR}(\nu_s(CD_2))$ indicates the absence of transverse ordering of the stearoyl chains, i.e., rotational symmetry about the chain long axis and/or nontilted chain axes with respect to the bilayer normal as was observed also for the palmitoyl chains in the L_β phase of POPC. The existence of the CH_2 wagging progression of fully proteated SDPC at small RH unequivocally gives evidence of the all-*trans* conformation of a predominant fraction of the stearoyl chains in the gel phase (not shown).

Also at higher temperatures, T > 15°C, both spectral parameters, S_θ(stearoyl) and COG($\nu_s(CD_2)$), change in a sigmoidal fashion, however, into the opposite direction when compared with the changes at T < 15°C (Fig. 2). A similar behavior was observed at the transition from a nonlamellar phase of inversely curved aggregates (water inside) into the lamellar L_α phase (Binder et al., 1999a). In

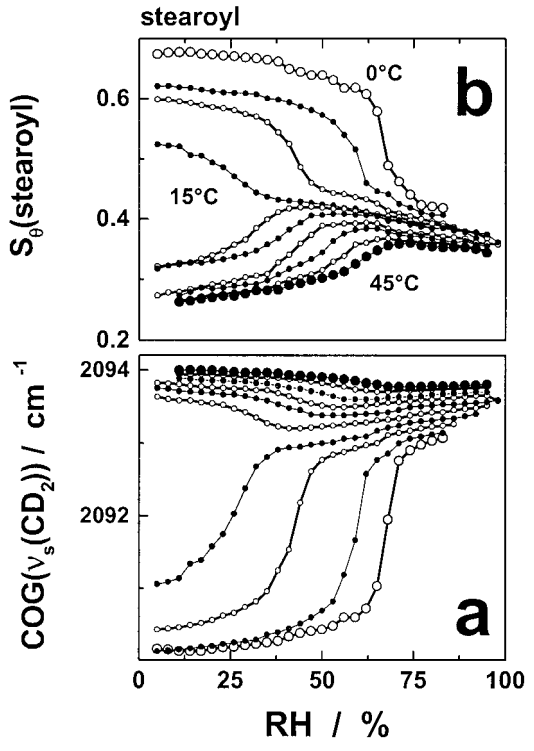

FIGURE 2 Center of gravity of the symmetric CD_2 stretching band (COG(ν_s(CD_2)); *a*) and longitudinal IR order parameter (S_θ; *b*) of the deuterated stearoyl chains of SDPC-d35 as a function of RH. The temperature of the hydration scans was increased from T = 0°C (○) to 45°C (●) in steps of 5 K.

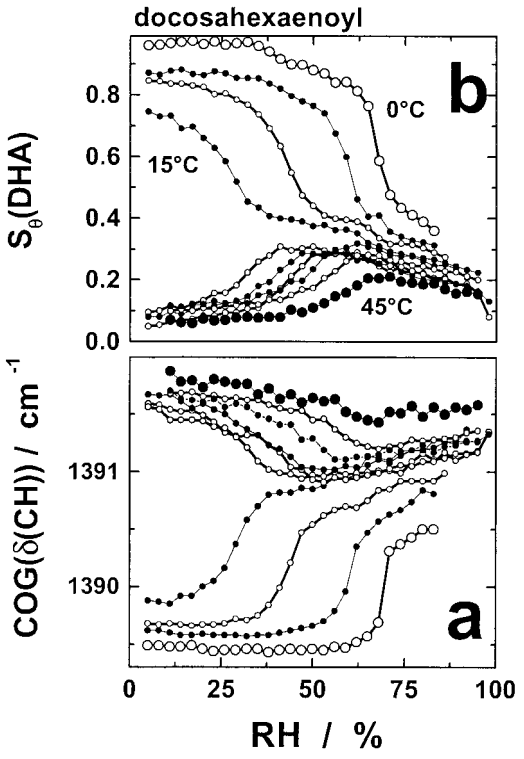

FIGURE 3 Center of gravity (COG(δ(CH)); *a*) and IR order parameter (S_{IR}(δ(CH)); *b*) of the C—H deformation mode of the vinyl groups of the DHA chains of SDPC-d35 as a function of RH. Conditions were as in Fig. 2.

this case the increase of S_θ reflects a change in the degree of membrane alignment at the solid surface, perhaps triggered by changes in aggregate morphology (see, e.g., Binder and Pohle, 2000). For example, the order parameter of aggregate morphology S_d (see Eq. 3) is expected to increase by the factor 4 when the system transforms from the H_{II} ($S_d(H_{II}) \approx 0.25$) into the lamellar phase ($S_d(lam) \approx 1$) (Binder et al., 1999a; Binder and Pohle, 2000). It is important to note that S_d scales the IR order parameters of all vibrational modes of the lipid, and thus the formation of nonlamellar structures is expected to reduce absolute S_{IR} values of other IR bands of SDPC-d35 as well.

Fig. 3 depicts the chain order parameter of the DHA chains, S_θ(DHA), and Fig. 4 the IR order parameter of the carbonyl and phosphate groups of SDPC-d35 as a function of RH. On the one hand, S_θ(DHA) suggests that the conformation and molecular order of the DHA chains vary in a similar fashion as the conformation and order of the saturated chains (Fig. 3 *b*). The phase transitions obviously involve the conformation and molecular order of the stearoyl and of the DHA chain.

In contrast, the S_{IR} values of the $\nu_{as}(PO_2^-)$ and the ν(C═O) bands of SDPC-d35 remain nearly constant under all conditions studied (Fig. 4). This result is important because it indicates that the macroscopic orientation of the lipids on the ATR crystal remains virtually unchanged, and thus the decrease of chain order parameters cannot be explained by formation of a nonlamellar phase. The observed variation of the IR order parameter of the methylene and vinyl groups predominantly originates from changes of the chain conformation. We suggest that a new lamellar phase with highly disordered chains forms at low RH and T > 15°C. It will be designated as L_α'.

The latter conclusion is confirmed by the center of gravity of the $\nu_s(CH_2)$ and δ(CH) bands, which change in a similar fashion as the respective IR order parameters (Figs. 1 *a*, 2 *a*, and 3 *a*). The mean frequencies of these modes are sensitive to the conformation of the saturated and polyunsaturated chains, respectively. The slightly higher mean frequency of the $\nu_s(CH_2)$ mode at small RH is compatible with a more disordered conformation of the polymethylene chains when compared with their conformation in the L_α phase. Direct proportionality between the $\nu_s(CH_2)$ frequency and the respective IR and ^{2}H-NMR order parameters was previously reported for fluid lipid membranes (Kodati and Lafleur, 1993; Le Bihan and Pezolet, 1998). Recently we found that COG($\nu_s(CH_2)$) is directly related to the mean area that the chain occupies in the membrane plane (Binder et al., 1999b). Hence, the IR frequencies are expected to reflect changes of the lateral packing of the acyl chains.

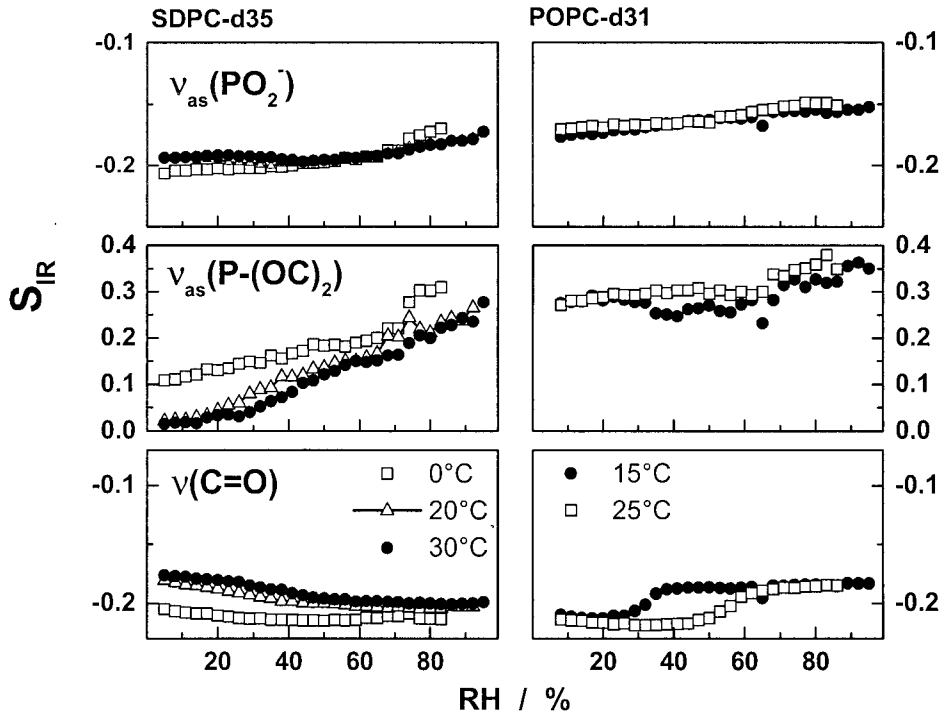

FIGURE 4 IR order parameters of the antisymmetric PO_2^- (*above*) and P-$(OC)_2$ (*middle*) stretching modes near 1230 cm^{-1} and 820 cm^{-1}, respectively, and of the C═O stretching band (*below*) near 1735 cm^{-1} of SDPC-d35 (*left*) and POPC-d31 (*right*) as a function of RH at different temperatures.

Water sorption characteristics

The lipids POPC and SDPC progressively hydrate with increasing RH as indicated by the increasing number of water molecules per lipid, $R_{W/L}$ (Fig. 5). Comparison of the sorption isotherms of both lipids (T = 25°C) shows that SDPC imbibes slightly more water at RH > 60% than POPC (Fig. 5). The step of the sorption isotherm of POPC at the L_β-L_α phase transition reflects a slightly increased hydration potency of the fluid phase (Binder et al., 1999e). No change of hydration behavior was observed at the L_α'-L_α phase transition of SDPC.

The interaction of water with the polar moieties of the lipid can be characterized by means of IR spectroscopy. For example, the mean frequency of the C═O stretching vibration of the carbonyl group, ν(C═O), can serve as a sensitive marker band that characterizes the hydration of the carbonyl groups in lipid assemblies (Binder et al., 1999a; Blume et al., 1988; Pohle et al., 1998). The center of gravity of the C═O band, COG(ν(C═O)), shifts typically toward smaller wave numbers upon hydration due to the formation of H bonds between the water and the carbonyl moieties (Fig. 6). The break of the

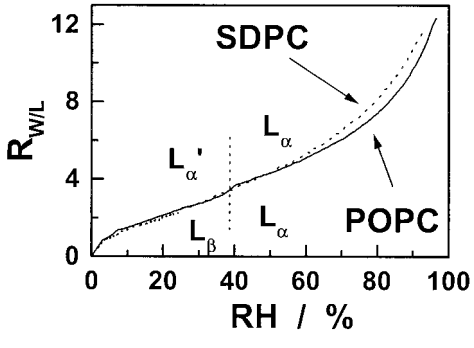

FIGURE 5 Molar water-to-lipid ratio, $R_{W/L}$, of SDPC and POPC as function of RH at T = 25°C. The vertical dotted line marks the L_β-L_α phase transition of POPC and the L_α'-L_α transition of SDPC, which occur in both lipids at virtually equal RH.

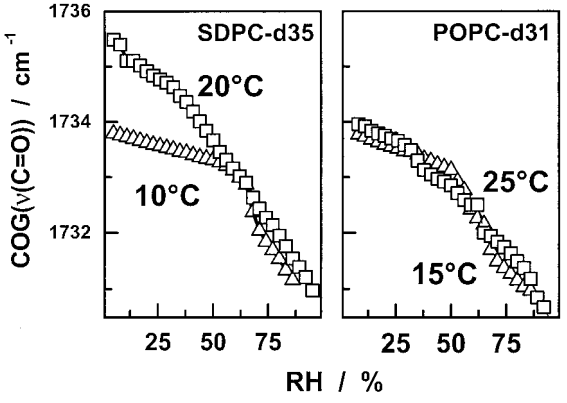

FIGURE 6 Center of gravity of the C═O stretching band of SDPC-d35 (*left*) and POPC-d31 (*right*) at two temperatures as a function of RH.

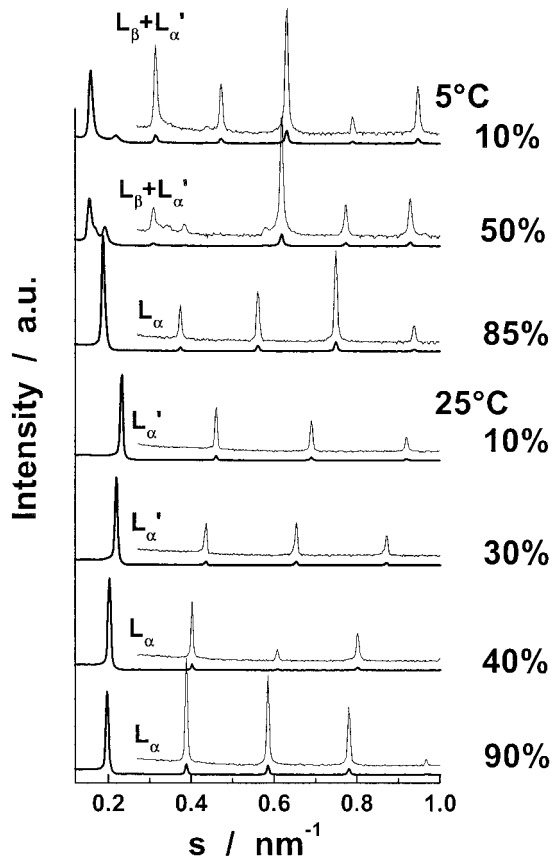

FIGURE 7 Representative x-ray diffraction pattern of SDPC-d35, which was measured at 5°C (*above*) and 25°C (*below*) at different RHs.

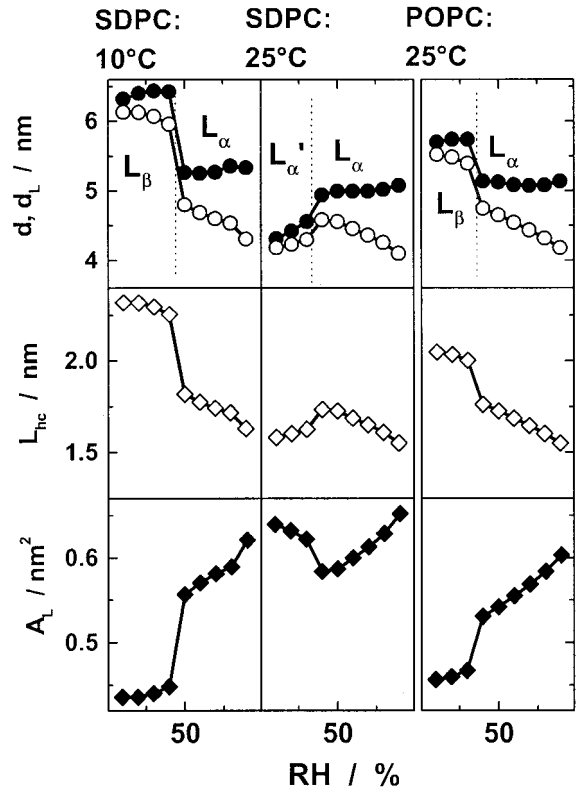

FIGURE 8 Dimensions of the SDPC and POPC bilayers as a function of RH at T = 10°C (SDPC) and 25°C (SDPC and POPC). ●, Repeat distance d; ○, thickness of the bilayer d_L; ◆, area per lipid A_L (Eq. 6); ◇, $L_{hc} = 0.5d_{hc}$, thickness of the hydrophobic core of one-half of the bilayer.

COG(ν(C═O)) graph at the onset of the chain melting transition of POPC was attributed to the increased water uptake of the carbonyl groups in the fluid L_α phase (Fig. 6 and Binder et al., 1999e). The mean ν(C═O) frequency of SDPC shows the same behavior at T < 15°C (see Fig. 6 for T = 10°C). The break of the COG(ν(C═O)) graph of SDPC disappears at T > 15°C (see Fig. 6 for T = 20°C). The carbonyl groups obviously dehydrate more strongly in the RH range that has been attributed to the L_α' phase when compared with the L_β phase. In other words, the progressively bigger COG(ν(C═O)) values of SDPC indicate that the carbonyls are more effectively screened from the water than in POPC membranes where a certain amount of water remains trapped near the C═O groups.

Interestingly, the IR absorption bands of the phosphate group of SDPC and POPC give no indication of different water binding characteristics of this moiety in the different phases (not shown). The strongly hygroscopic character of the phosphate group obviously prevents significant modifications of its hydration by changes of chain ordering in the investigated systems.

Small-angle x-ray diffraction characteristics of SDPC

X-ray diffractograms of SDPC show a strong first-order Bragg peak and a series of weak, equally spaced peaks up to fifth order (see Fig. 7). This result confirms the existence of multibilayer stacks at all conditions studied. The lamellar gel phase (L_β) in most cases coexists with a second lamellar phase that shows the characteristics of L_α' (see below). The intensity of the respective Bragg peaks decreases distinctly after equilibration of the samples for 12 h. We conclude that the gel corresponds to thermodynamic equilibrium whereas L_α' is metastable at RH < 50% and T < 15°C. Only diffractograms that were measured within 10 h after preparation of the lipid films were considered for further analysis because of potential degradation of the DHA chains at a longer time.

The repeat distance of SDPC-d35 in the L_α phase is nearly independent of RH (Fig. 8). However, it decreases considerably with hydration in the L_α' phase. The gel phase of the lipids is characterized by distinctly bigger d values in comparison with those of the fluid systems owing to the stretched conformation of the chains (vide infra).

Bilayer dimensions

The mean dimensions of the membranes were estimated by means of the simple approach of nonpenetrating lipid/water layers proposed by Luzzati (1968) (Fig. 8). Removal of water from the lipid layers decreases the mean area per lipid, A_L, in the L_α and in the L_β phase. That means the lipid bilayers contract laterally upon dehydration. The nearly constant repeat distance shows that the reduction of the interbilayer water gap is almost entirely compensated by the thickening of the bilayers.

In sharp contrast to this behavior, the bilayers expand laterally and contract vertically in the L_α' phase upon further dehydration. This result seems to be quite atypical. In the discussion section we propose a molecular interpretation for this behavior. Comparison of the dimensions of SDPC and POPC membranes shows that at identical hydration levels in the L_α phase, area per lipid increases with the number of double bonds in the *sn*-2 chain. The same behavior was observed when comparing stearoyloleoylphosphatidylcholine (SOPC) with SDPC (Koenig et al., 1997).

Characterization of the L_α' phase using ^{31}P and ^2H NMR

The ^{31}P NMR spectra of SDPC were recorded over the temperature range 0–50°C. The sample containing excess water was in the L_α phase, characterized by an anisotropy of chemical shift of −45 ppm at the temperature of 40°C (see Fig. 9 *a*). The sample prepared at RH of 33% had a phase transition into the L_α' phase at T ≈ 15°C, in good agreement with the IR measurements. The ^{31}P anisotropy of chemical shift of L_α' is considerably smaller than the value of L_α, just −34 ppm at 40°C. The small peak to higher field from the 90° orientation shoulder is most likely caused by the presence of a few percent of an L_α phase (Fig. 9 *a*).

Not only the ^{31}P anisotropy of chemical shift was smaller in the L_α' phase but also the ^2H NMR quadrupolar splittings of the stearic acid hydrocarbon chains. The spectra and the corresponding smoothed chain order parameter profiles are shown in Fig. 9, *b* and *c*. Hydrocarbon chains in both the L_α and L_α' phases have an order parameter plateau in the first half of the chain near the glycerol. Order in the second half of the chain decreases rapidly toward the bilayer center. In first approximation both order parameter profiles differ from each other by a constant factor of 1.33 with lower order in the L_α' phase (see Fig. 9 *c*).

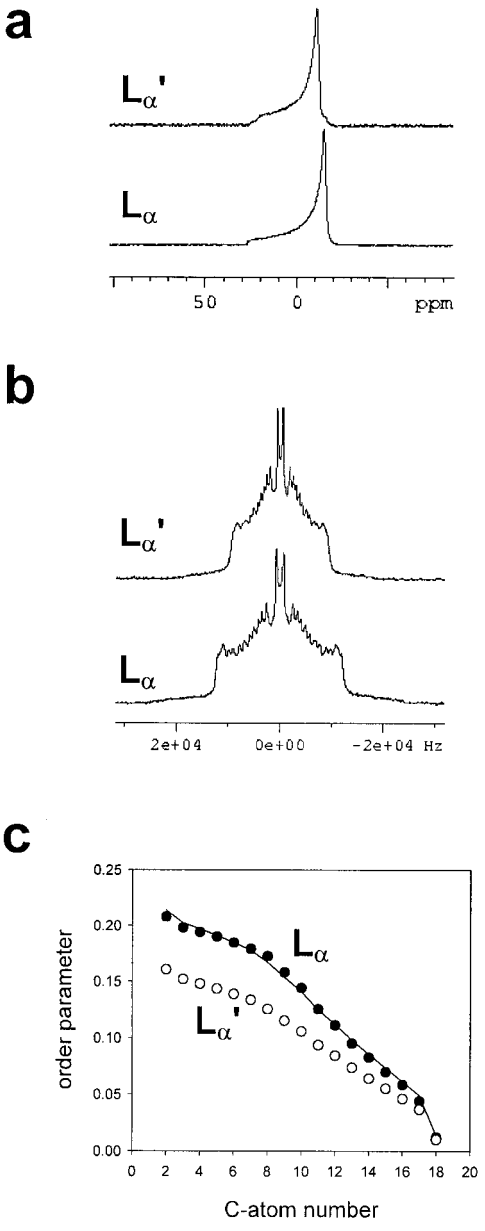

FIGURE 9 NMR characteristics of *sn*-1 chain perdeuterated SDPC-d35. Proton-decoupled ^{31}P NMR (*a*) and ^2H NMR (*b*) powder spectra in the L_α (*below*, hydrated with 50 wt % water, T = 40°C) and L_α' phase (*above*, RH = 33%, T = 40°C). ^{31}P NMR line shapes are characteristic for liquid-crystalline lamellar phases. The anisotropy of chemical shift in the L_α phase (−45 ppm) is larger than the anisotropy of chemical shift of the L_α' phase (−34 ppm). ^2H NMR quadrupolar splittings of stearic acid methylene segments is considerably smaller in the L_α' phase compared with the L_α phase. (*c*) Respective smoothed S_{CD} order parameter profiles in the L_α (●) and L_α' (○) phases calculated from ^2H NMR quadrupolar splittings of the stearic acid chains. The solid line in *c* represents L_α'order parameters multiplied by a factor of 1.33.

DISCUSSION

RH-T phase diagrams

On the basis of the phase transition data of the FTIR and x-ray diffraction experiments, we are able to construct the RH-T phase diagrams of SDPC and POPC (Fig. 10). The substitution of H_2O by D_2O does not significantly affect the phase transitions. Deuteration of the *sn*-1 chain in SDPC-d35 shifted the L_β-L_α phase transition by 2–4 K to lower temperature. Both lipids have a lyotropic chain melting

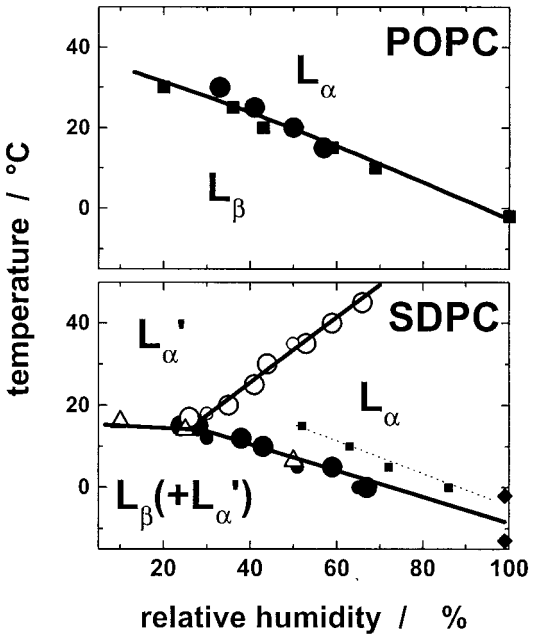

FIGURE 10 RH-T phase diagram of SDPC-d35 (*below*) and POPC-d31 (*above*). The solid and open circles are obtained from the center points of the sigmoidal changes of the IR spectral parameters at the L_β-L_α and L_α'-L_α phase transitions, respectively. The larger symbols correspond to hydration experiments with H_2O and the smaller ones to D_2O. Hydration and dehydration scans show no significant hysteresis. The transition data of SDPC-d35 in excess water were taken from Holte et al. (1995) (♦). ■, L_β-L_α phase transitions of the proteated species, SDPC and POPC; △, transition data of temperature scans at constant RH.

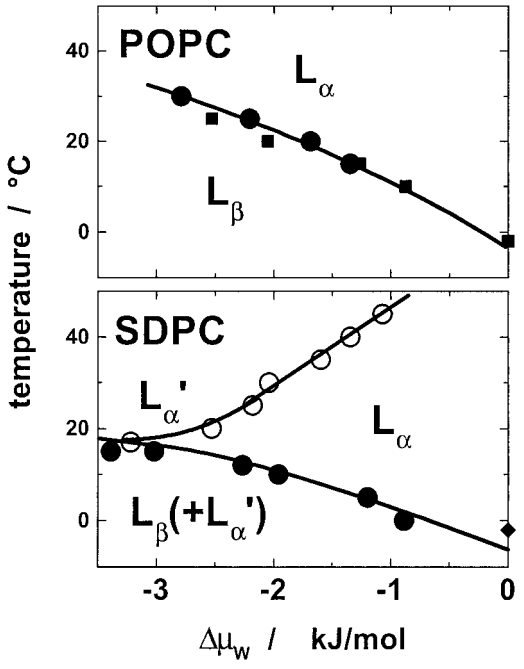

FIGURE 11 $\Delta\mu$-T phase diagram of SDPC-d35 (*below*) and POPC-d31 (*above*).

transition between the L_β and L_α phases. Its temperature increases almost linearly with decreasing RH. Lyotropic chain melting transitions of lipids with PC headgroups have been well studied previously (Binder et al., 1999e; Janiak et al., 1979; Jürgens et al., 1983; Pohle et al., 1998), and their existence in SDPC and POPC water dispersions is not surprising.

In contrast to the monounsaturated POPC, polyunsaturated SDPC converts to a liquid-crystalline lamellar phase, L_α', at higher temperatures and/or lower hydration. The existence of a second lamellar phase at these conditions was not expected. Because dehydration causes a reduction of the headgroup volume, phosphatidylcholines typically form nonlamellar phases of inverse symmetry at low hydration and higher temperatures with a high degree of negative curvature strain in their monolayers. For example, mono- and dihydrates of disaturated PCs (di-C14, di-C16, and di-C18) transform from the gel state to nonlamellar phases of ribbon-like (P_δ), cubic (Q_α), and/or inverse hexagonal (H_{II}) symmetry at $T > 60°C$ (Dörfler and Brezesinski, 1983; Janiak et al., 1979; Jürgens et al., 1983). A L_α-to-nonlamellar transition of nearly dry POPC (RH < 15%) was found at $T > 30°C$ (Binder, unpublished results). Dioleoyl PC (DOPC) exhibits this event upon dehydration at room temperature near RH ≈ 40% (Binder et al., 1999d). Interestingly, a lyotropic phase transition between two lamellar liquid-crystalline phases was found for 1,2-diphytanoyl-3-glycero PC (DPhPC), which possesses branched methylene groups in each of the hydrocarbon chains (Hsieh et al., 1997). Also, DPhPC membranes expand laterally at low RH (He et al., 1996). This similarity with SDPC suggests existence of a common underlying molecular mechanism.

The L_β-L_α' transition temperature is virtually independent of water chemical potential at RH < 30%. This was measured by means of temperature scans at constant RH (triangles; IR data are not shown). Hydration/dehydration scans at constant temperature do not detect this phase transition.

Thermodynamics of the lyotropic phase transitions

The RH-T phase diagram can be transformed to a $\Delta\mu_W$-T representation (see Fig. 11) where

$$\Delta\mu_W \equiv \mu_W(\mathrm{RH}) - \mu_W^{\mathrm{bulk}} = RT \times ln(RH/100\%) \quad (8)$$

is the difference of the chemical potential of water adsorbed to the lipid at a given RH and bulk water, $\mu_W^{\mathrm{bulk}} = \mu_W(\mathrm{RH} = 100\%)$. R denotes the gas constant. The chemical potential is defined as the partial molar Gibbs free energy of water in the two-component mixture (water plus lipid), $\mu_W \equiv \partial G/\partial R_{W/L}$ (G is the Gibbs free energy per mole of lipid). The slope of the transition lines in the $\Delta\mu_W$-T phase

TABLE 1 Partial molar values of the thermodynamic functions at the phase transitions

Phase transition	$-\Delta\mu_w$ range*	POPC		SDPC	
		$T\Delta s_w$	Δh_w	$T\Delta s_w$	Δh_w
L_β/L_α	0–1.7	23 ± 3	24 ± 3	31 ± 3	32 ± 3
	1.7–3.0	52 ± 10	54 ± 10	67 ± 10	69 ± 10
L_α'/L_α	1–2.5			−17 ± 10	−15 ± 10
	2.5–3.0			−47 ± 10	−44 ± 10
L_β/L_α'	3.0–4.0			320 ± 50	330 ± 50

All data are given in units of kJ/mol.
*Slopes are obtained by regression lines in the respective range of $\Delta\mu$.

diagram is directly related to the difference of the partial molar entropy (and partial molar enthalpy) of water at the phase transition and the molar entropy (and enthalpy) of bulk water (see Appendix and Binder et al., 2000):

$$\frac{d\Delta\mu_W^{tr}}{dT} = -\Delta s_W^{tr} = \frac{\Delta\mu_W^{tr} - \Delta h_W^{tr}}{T}, \qquad (9)$$

with $\Delta s_W^{tr} = s_W(RH^{tr}) - s_W^{bulk}$ ($s_W \equiv \partial S/\partial R_{W/L}$) and $\Delta h_W^{tr} = h_W(RH^{tr}) - h_W^{bulk}$ ($h_W \equiv \partial H/\partial R_{W/L}$; S and H are the entropy and enthalpy per mole of lipid, respectively; see also Binder et al., 1999e). In other words, the $\Delta\mu_W$-T phase diagram yields information about the change of Gibbs free energy, entropy, and enthalpy that accompanies the adsorption of water at the respective phase transition. The results of this analysis for two hydration ranges can be summarized as follows (see Table 1):

1) The different sign of the slopes of the L_α'-L_α and L_β-L_α transition lines clearly indicate that the hydration-induced chain melting transition is driven by entropy whereas the transition between the L_α' and L_α phase is driven by enthalpy. Chain melting is endothermic because the system loses energy owing to weaker dispersion forces between the acyl chains and/or because of energetically less favorable conformations of the acyl chains in the fluid phase (vide infra). Contrarily, at the L_α'-L_α transition the interchain interaction energy obviously gains due to denser lateral packing and increased chain ordering in L_α membranes.

2) The enthalpy and entropy changes compensate each other nearly completely. For example, the weakening of molecular interactions of the gel phase at the chain melting transition transforms into molecular disorder in the fluid state to a high degree. Note that the alteration of composition owing to the adsorption of water is accompanied by the change of Gibbs free energy, and thus enthalpy-entropy compensation is not required in the thermodynamic process studied (Binder et al., 1999e)

3) The partial molar quantities are defined as the change of enthalpy/entropy upon differential adsorption of water. Their absolute values increase considerably with decreasing water activity. In other words, the more direct a water molecule interacts with the lipid, the stronger it affects the properties of the water and lipid. This tendency appears plausible because the interaction strength of water with the PC moieties is expected to increase with dehydration (Binder et al., 1999e; Rand and Parsegian, 1989).

4) Δh_W and $T\Delta s_W$ of SDPC are significantly bigger than those of POPC. That means that adsorption of a water molecule to the polyunsaturated lipid more strongly affects the enthalpy and entropy of the system than adsorption of the same amount of water to the monounsaturated lipid. In a more general context, this result shows that perturbing a membrane of polyunsaturated lipids affects a wider range of entropic and energetic (i.e., enthalpic) states than a similar perturbation of lipids with monounsaturated and/or saturated chains. This difference between the mono- and polyunsaturated lipids becomes clearly evident at smaller RH at which SDPC transforms from the L_β into the L_α' phase with increasing T. The virtually horizontal transition line between the L_β and L_α' phase is equivalent to relatively big absolute values of $T\Delta s_W$ and Δh_W (Table 1). The change of systems enthalpy upon transformation between the solid and fluid phases is given in a first-order approximation by the endothermic heat of chain melting, and thus it can be assumed to be virtually similar for both melting transitions, $\Delta H^{L\beta\rightarrow L\alpha} \approx \Delta H^{L\beta\rightarrow L\alpha'}$. Consequently, the considerably bigger partial molar enthalpy of water at the L_β/L_α' transition, $\Delta h_W^{L\beta\rightarrow L\alpha'} \equiv \Delta H^{L\beta\rightarrow L\alpha'}/\Delta R_{W/L}^{L\beta\rightarrow L\alpha'} \gg \Delta h_W^{L\beta\rightarrow L\alpha} \equiv \Delta H L\beta\rightarrow L\alpha/\Delta R_{W/L}^{L\beta\rightarrow L\alpha} > 0$, must be attributed to a considerably smaller increase of hydration, $\Delta R_{W/L}^{L\beta\rightarrow L\alpha'} \ll \Delta R_{W/L}^{L\beta\rightarrow L\alpha}$. Indeed, the mean frequency of the C═O stretching band, COG(ν(C═O)) (Fig. 6), indicates a relatively weak degree of hydration of the carbonyl region in the L_α' phase compared with that in the L_α phase.

Solid membranes of SDPC seem to be less stable than membranes of disaturated and monounsaturated lipids under identical conditions. Information on phase transition temperatures of fully hydrated lipids supports this view. The substitution of *cis* monounsaturated C18:1ω9 chain for stearoyl chain in the *sn*-2 position of di-C18:0 PC brings the depression of main phase transition temperature, T_m, by 58 K (Holte et al., 1995; Ichimori et al., 1998). An additional *cis* double bond in the *cis*-di-unsaturated chain of C18:0/C18:2ω6-PC decreases T_m further by ~13 K. A third double bond in C18:0/C18:3ω3-PC has nearly no additional effect on T_m. Also, longer polyunsaturated chains such as the DHA chain in SDPC (C18:8/C22:6ω3-PC) leave T_m nearly unchanged when compared with C18:0/C18:2ω6 PC. These facts seem to indicate that the conditions of chain melting/freezing of saturated-polyunsaturated mixed-chain lipids are mainly determined by the saturated chains. With respect to chain melting, the polyunsaturated chains appear to weaken the mean field dispersion energy in the hydrophobic core of the bilayer. A similar conclusion was previously drawn on the basis of an analysis of chain ordering in polyunsaturated C16/C22:ω6 PC (Salmon et al., 1987). On the other hand, the transition temperature also remains vir-

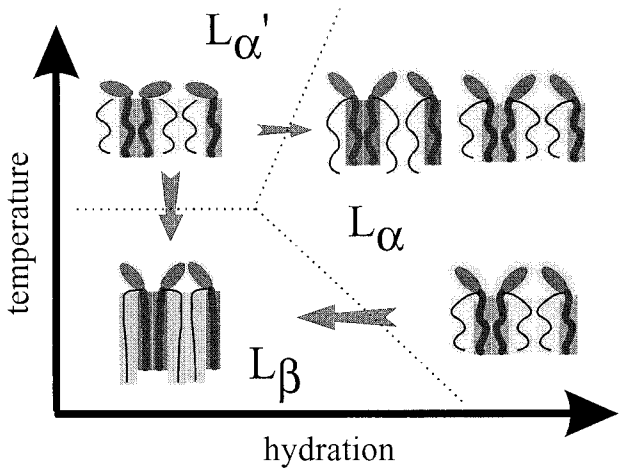

FIGURE 12 Schematic illustration of the different phases of SDPC. The arrows across the phase boundaries (···) point in the direction of increasing chain ordering. Saturated and polyunsaturated chains are indicated by thick and thin lines, respectively. Only one monolayer of the bilayer is shown. See text for details.

tually unchanged after substituting the stearoyl chain by a palmitoyl one in C16:0/C18:2ω6 PC ($T_m \approx -3$°C (Litman et al., 1991)). Hence, the polyunsaturated chains also to some degree contribute to the stability of the lamellae.

Molecular origin of the lyotropically induced gel phase

The cohesive interfacial tension at the hydrocarbon/water interface tends to contract the membrane area. Repulsive forces between neighboring lipids due to steric and entropic effects in the polar and apolar parts of the bilayer counterbalance the attractive forces at the interface. Desorption of water from the lipid assemblies results in an additional lateral tension that compresses lipid bilayers (Koenig et al., 1997). In a simplified view, this effect can be rationalized by the fact that neighboring lipids can approach each other more closely after removing water from the polar region of the bilayer. As a consequence, the area per lipid molecule decreases with dehydration in the L_α phase (Fig. 8). The reduction of the average cross-sectional area of the lipids is paralleled by an increase of the mean length of their acyl chains, L_{hc} (Fig. 8), and an increase of the longitudinal chain order parameters, S_θ (Figs. 1 *b*, 2 *b*, and 3 *b*). A denser lateral arrangement of acyl chains causes lowering of the mean (negative) dispersion energy between the chains that is roughly proportional to the longitudinal chain ordering. The shift of the center of gravity of the methylene stretches to smaller wave numbers reflects this tendency (Binder et al., 1999b) (Figs. 1 *a* and 2 *a*). At a critical value of the chemical potential of water, POPC and SDPC (at $T < 15$°C) undergo the lyotropic transition from the L_α into the L_β phase. At the transition, the chains convert to a more extended conformation (see also Fig. 12 for illustration). The appearance of the methylene wagging band progression in the spectra of proteated POPC and SDPC in the gel phase provides unambiguous evidence that the all-*trans* conformation of saturated chains is predominant (data not shown). The half-width of the hydrophobic core of POPC and SDPC bilayers, $L_{hc} \approx 2.0$ nm and 2.3 nm, respectively, slightly exceeds the length of the corresponding saturated chains in the all-*trans* conformation, $L_{max} \approx 1.91$ nm (palmitoyl) and 2.16 nm (stearoyl), calculated by $L_{max} \approx n_{CH2} \cdot 0.127$ nm (n_{CH2} is the number of methylene groups per chain). Note that the length of extended conformations of the DHA chain, such as the angle iron (2.26 nm) and helical (2.27 nm) conformation (Jandacek and Broering, 1989), are comparable with L_{hc} of SDPC in L_β phase.

Upon transformation into the gel state, the mean thickness of the hydrophobic core of SDPC bilayers increases by ~25% whereas the thickness of POPC membranes increases only by ~12% (Fig. 8). Hence, membranes of polyunsaturated SDPC deform more drastically at this event compared with bilayers of monounsaturated POPC. Presumably these differences are a reflection of the differences in conformational degrees of freedom between saturated, monounsaturated, and polyunsaturated chains

Possible molecular interpretation of the L_α' phase

A new lamellar phase called L_α' forms upon dehydration of SDPC at $T > 15$°C. It is characterized by a larger area per lipid molecule compared with the preceding L_α phase. The lamellae expand laterally with dehydration in this novel lamellar phase. Hence, the removal of water effectively decreases the absolute value of lateral tension. That means the decrease of volume of the polar region must be overcompensated by a considerable change of membrane architecture that increases the cross section of the lipid molecules.

This unusual behavior may have been caused by substantial interdigitation of the acyl chains from both leaflets of the bilayer. Several arguments strongly contradict this explanation. 1) The area increase of $\Delta A_L < 0.05$ nm^2 is considerably smaller than the minimum cross section of a chain, $a_{min} > 0.18$ nm^2; one would expect $\Delta A_L \approx 2a_{min}$ (Pascher et al., 1992). 2) Interdigitation typically appears in solid lipid phases with increasing hydration and not with dehydration of fluid bilayers (Kim et al., 1987). 3) Last but not least, the observed decrease of chain order parameters appears to be in conflict with chain interdigitation that is expected to increase order parameters. Also, one would expect a substantial change in the chain order profile. However, the ^{2}H NMR experiments reveal that the shape of the order parameter profile has not changed in first approximation. All segmental order parameters of the L_α' phase could be recalculated into order parameters of the L_α phase by

multiplication with a constant (see Fig. 9 *c*). This indicates that order parameters of the entire saturated hydrocarbon chain have decreased, making interdigitation unlikely.

In a previous study we observed a preferential increase in length of the polyunsaturated DHA chain in the L_α phase with dehydration (Koenig et al., 1997). One can expect that this results in substantial differences of average chain length between the saturated and polyunsaturated hydrocarbon chains in the bilayer. Such difference may cause unfavorable packing arrangements of the chains in the bilayer center including formation of voids that are energetically unfavorable and thus destabilize the L_α phase. (see Fig. 12). Alternatively, one could imagine that conformational restrictions within the fluid DHA chains prevent the SDPC molecule from occupying a mean area below a critical value of A_L.

In addition to restrictions in area reduction, lipid molecules with polyunsaturated DHA chains must be capable of reorganizing water molecules in their first hydration shell at low values of the chemical potential of water to enable the sudden increase in area per molecule and the corresponding decrease in water layer thickness. One could envision that the polarizability of double bonds enables these phosphocholine molecules to partially expose the polyunsaturated chains in the water.

Indeed, the IR order parameter of the ν_{as}(P-$(OC)_2$) mode and the NMR measurements of the ^{31}P anisotropy of chemical shift reveal that the phosphate groups of SDPC and POPC (T = 25°C) behave in a different fashion upon dehydration at RH < 50% (see Fig. 4), confirming the involvement of the lipid-water interface in the L_α-L_α' transition of SDPC. The transition moment of the antisymmetric stretches of the (CO)—P—(OC) fragment orients roughly along the interconnecting line between the two esterified oxygens (Binder et al., 1998). The distinct decrease of $S_{IR}(\nu_{as}$(P-$(OC)_2))$ in the L_α' phase indicates that the long axis of the phosphate groups aligns, on average, more parallel to the membrane plane. Isotropic disordering can be excluded as an explanation because other IR order parameters of the phosphate group such as $S_{IR}(\nu_{as}(PO_2^-))$ remain virtually unaffected (see Fig. 4). Such a change in average headgroup orientation is the likely cause for the reduction in the effective ^{31}P anisotropy of chemical shift that was measured by NMR. The NMR data also indicate that the headgroup maintains a fair amount of motional degrees of freedom at the low water content, eliminating the possibility of formation of a rigid headgroup environment.

A subtle decrease of the absolute values of the IR order parameters of the carbonyl groups, $S_{IR}(\nu$(C═O)), indicates a slightly more disordered polar region of SDPC in the L_α' phase (Fig. 4). The tendency of the acyl chains to align parallel in membranes of diacyl 1,2-glycero-phospholipids forces a 90° bend of the *sn*-2 chain axis near the C2 position whereas the *sn*-1 chain adopts an extended conformation near the glycerol. The existence of a similar bend for DHA chains in the *sn*-2 position was predicted in simulations (Applegate and Glomset, 1986). However, weaker dispersion forces in the hydrophobic core of membranes of polyunsaturated SDPC are expected to decrease conformational restrictions in the region near the glycerol group. The linear dichroism of the antisymmetric CO-O-C ester bond stretching vibration reveals lower order of this moiety in the L_α' phase (data not shown, manuscript in preparation). Hence, the higher degree of conformational freedom of this chain region in SDPC enables lipid packing with larger area per molecule.

DPhPC forms a lamellar phase that laterally expands upon dehydration, similar to the L_α' phase of SDPC. It was argued that the packing geometry near the headgroup region plays a crucial role in the dehydration-induced expansion of the membranes (Hsieh et al., 1997). The authors suggested that the relatively large cross-sectional area of DPhPC (0.76–0.80 nm^2 at RH = 100%) may enable interdigitation of the PC headgroups of adjacent bilayers in multibilayer stacks. We do not believe that this interpretation applies to SDPC membranes, because the phosphate groups, on average, adopt a more in-plane orientation in the L_α' phase (vide supra) and because of the relatively small lateral area per lipid of 0.62–0.64 nm^2 (see Fig. 8) compared with DPhPC. A detailed analysis of headgroup orientation using IR linear dichroism data will be given elsewhere.

In summary, unfavorable arrangement of the chains in the bilayer center and/or restricted conformations of the polyunsaturated chains in combination with altered properties of SDPC at the lipid/water interface enable the transition to a novel liquid-crystalline lamellar phase state with larger area per molecule, shorter effective length of hydrocarbon chains, and, consequently, lower degree of molecular order.

SUMMARY AND CONCLUSIONS

We studied the lyotropic phase behavior of SDPC to probe the specific properties of polyunsaturated lipids in biological membranes. At full hydration and temperatures above 0°C, SDPC forms a liquid-crystalline L_α phase. Dehydration induces a gel (L_β) phase at T < 15°C in analogy to the phase behavior of monounsaturated POPC that has been investigated for sake of comparison. Dehydration at T > 15°C causes a phase transition into a novel lamellar liquid-crystalline phase called L_α'. The L_α'-L_α transition is driven by enthalpy contrary to the L_β-L_α transformation that is driven by entropy.

L_α' bilayers exhibit the unusual tendency to expand laterally and to contract vertically upon water removal from the polar region of the membranes. We suggest that this surprising behavior of the new lamellar phase reflects specific conformations and/or interactions of polyunsaturated lipid hydrocarbon chains when paired with saturated polymethylene chains. Their phase properties differ considerably from those of disaturated and monounsaturated lipids.

Our results suggest that lipid polyunsaturation is important for biological systems because of altered physicochemical properties as shown here for SDPC. Characterization of membranes in terms of fluidity or local ordering, which was provided previously, may be inadequate to completely describe the role of polyunsaturated acyl chains. We suggest that a comprehensive description should take into account specific conformational properties of the polyunsaturated chains. In this study, IR linear dichroism was successfully applied to detect phase transitions. Detailed analysis of IR linear dichroism of selected absorption modes of DHA chains in membranes, in combination with ^{2}H NMR order parameter analysis, NMR cross-relaxation experiments, and molecular dynamics simulations of the polyunsaturated chains are expected to open new insights into the conformational degrees of freedom of DHA in the lipid matrix. Results will be presented in forthcoming publications.

We thank Ms. U. Dietrich for performing the x-ray measurements, Dr. J. Schiller for verifying lipid purity by MALDI-TOF mass spectroscopy, Dr. W. Teague for preparation of the NMR samples, and Mr. J. Mathews for verifying lipid purity by GC.

This work was supported by the Deutsche Forschungsgemeinschaft, SFB 197 (TP A10).

APPENDIX

Derivation of Eq. 9

The Gibbs free energy of a binary lipid-water mixture per mole of lipid is $G = \mu_L + R_{W/L}\mu_W$, where μ_L and μ_W denote the chemical potentials of lipid and water, respectively. The complete differential, $dG = d\mu_L + R_{W/L}d\mu_W + \mu_W dR_{W/L}$, can be set equal to the change of G at isobaric conditions, $dG = -SdT + \mu_W dR_{W/L}$, to obtain the Gibbs-Duhem relation, $d\mu_L = -SdT - R_{W/L}d\mu_W$, or equivalently,

$$d\mu_L/dT = -S - R_{W/L}d\mu_W/dT \qquad (10)$$

Here, S denotes the entropy of the system per mole of lipid. The chemical potentials of the components in two coexisting phases are equal at the phase boundary, i.e., $\mu_i^{tr} = \mu_i^1 = \mu_i^2$, or equivalently, $d\mu_i^{tr}/dT = d\mu_i^1/dT = d\mu_i^2/dT$ ($i = L, W$; the superscripts 1 and 2 refer to the two phases that coexist at the transition, tr). With Eq. 10 one obtains the Clausius-Clapeyron equation:

$$\frac{d\mu_W^{tr}}{dT} = -\frac{S^2 - S^1}{R_{W/L}^2 - R_{W/L}^1} \qquad (11)$$

This derivation is similar to Hung et al. (2000). The right term in Eq. 11 represents the ratio of the entropy difference between both phases and the respective difference of moles of water adsorbed per mole of lipid. It is just the partial molar entropy of water at the phase transition, $s_W^{tr} = (S^2 - S^1)/(R_{iW/L}^2 - R_{W/L}^1)$. Finally, Eq. 11 transforms into Eq. 9 given above after considering bulk water as the reference state ($\mu_W = \mu_W^{bulk} + \Delta\mu_W$; $s_W = s_W^{bulk} + \Delta s_W$) and after making use of the elementary relation $d\mu_W^{bulk}/dT = -s_W^{bulk}$.

REFERENCES

Albrand, M., J.-F. Pageaux, M. Lagarde, and R. Dolmazon. 1994. Conformational analysis of isolated docosahexanoic acid (2:6 n-3) and its 14 (S) and 11 (S) hydroxy derivatives by force field calculations. *Chem. Phys. Lipids.* 72:7–17.

Applegate, K. R., and J. A. Glomset. 1986. Computer-based modelling of the conformation and packing properties of docosahexanoic acid. *J. Lipid Res.* 27:658–680.

Binder, H. 1999. Infrared dichroism investigations on the acyl chain ordering in lamellar structures. III. Characterisation of the chain tilt and biaxiality in the solid phases of dipalmitoylphosphatidylcholine as a function of temperature and hydration using molecular order parameters. *Vibration. Spectrosc.* 21:151–163.

Binder, H., A. Anikin, B. Kohlstrunk, and G. Klose. 1997. Hydration induced gel states of the dienic lipid 1,2-bis(2, 4-octadecanoyl)-*sn*-glycero-3-phosphorylcholine and their characterization using infrared spectroscopy. *J. Phys. Chem. B.* 101:6618–6628.

Binder, H., A. Anikin, G. Lantzsch, and G. Klose. 1999a. Lyotropic phase behavior and gel state polymorphism of phospholipids with terminal diene groups: infrared measurements on molecular ordering in lamellar and hexagonal phases. *J. Phys. Chem. B.* 103:461–471.

Binder, H., U. Dietrich, M. Schalke, and H. Pfeiffer. 1999b. Hydration induced deformation of lipid aggregates before and after polymerization. *Langmuir.* 15:4857–4866.

Binder, H., T. Gutberlet, and A. Anikin. 1999c. Biaxial ordering of terminal diene groups in lipid membranes an infrared linear dichroism study. *J. Mol. Struct.* 510:115–131.

Binder, H., T. Gutberlet, A. Anikin, and G. Klose. 1998. Hydration of the dienic lipid dioctadecadienoylphosphatidylcholine in the lamellar phase: an infrared linear dichroism and x-ray study on headgroup orientation, water ordering, and bilayer dimensions. *Biophys. J.* 74:1908–1923.

Binder, H., and B. Kohlstrunk. 1999. Infrared dichroism investigations on the acyl chain ordering in lamellar structures. II. The effect of diene groups in membranes of dioctadecadienoylphosphatidylcholine. *Vibration. Spectrosc.* 21:75–95.

Binder, H., B. Kohlstrunk, and H. H. Heerklotz. 1999d. A humidity titration calorimetry technique to study the thermodynamics of hydration. *Chem. Phys. Lett.* 304:329–335.

Binder, H., B. Kohlstrunk, and H. H. Heerklotz. 1999e. Hydration and lyotropic melting of amphiphilic molecules: a thermodynamic study using humidity titration calorimetry. *J. Colloid Interface Sci.* 220: 235–249.

Binder, H., B. Kohlstrunk, and W. Pohle. 2000. Thermodynamic and kinetic aspects of lyotropic solvation-induced transitions in phosphatidylcholine and phosphatidylethanolamine assemblies revealed by humidity titration calorimetry. *J. Phys. Chem. B.* 104:12049–12055.

Binder, H., and W. Pohle. 2000. Structural aspects of lyotropic solvation-induced transitions in phosphatidylcholine and phosphatidylethanolamine assemblies revealed by infrared spectroscopy. *J. Phys. Chem. B.* 104:12039–12048.

Binder, H., and H. Schmiedel. 1999. Infrared dichroism investigations on the acyl chain ordering in lamellar structures. I. The formalism and its application to polycrystalline stearic acid. *Vibration. Spectrosc.* 21: 51–73.

Blume, A., W. Hübner, and G. Messner. 1988. Fourier transform infrared spectroscopy of ^{13}C═O-labeled phospholipids: Hydrogen bonding to carbonyl groups. *Biochemistry.* 27:8239–8249.

Crawford, M. A., A. G. Hassam, G. Williams, and W. Whitehouse. 1977. Fetal accumulation of long-chain polyunsaturated fatty acids. *Adv. Exp. Med. Biol.* 83:135–143.

Dörfler, H.-D., and G. Brezesinski. 1983. Phase transformations in lecithin/water systems: the effect of water on phase transitions of lecithin/water monohydrates (germ.). *Colloid Polymer Sci.* 261:286–292.

Everts, S., and J. H. Davis. 2000. ^{1}H and ^{13}C nuclear magnetic resonance of multilamellar dispersions of polyunsaturated (12:6) phospholipids. *Biophys. J.* 79:885–897.

Harrick, N. J. 1967. Internal Reflection Spectroscopy. Wiley, New York.

He, K. S., W. T. Ludke, S. J. Heller, and H. W. Huang. 1996. Mechanism of alamethicin insertion into lipid bilayers. *Biophys. J.* 71:2669–2679.

Holte, L. L., S. A. Peter, T. M. Sinnwell, and K. Gawrisch. 1995. ^{2}H nuclear magnetic resonance order parameter profiles suggest a change of molecular shape for phosphatidylcholines containing a polyunsaturated acyl chain. *Biophys. J.* 68:2396–2403.

Hsieh, C.-H., S.-C. Sue, P.-C. Lyu, and W.-G. Wu. 1997. Membrane packing geometry of diphytanoylphosphatidylcholine is highly sensitive to hydration: phospholipid polymorphism induced by molecular rearrangement in the headgroup region. *Biophys. J.* 73:870–877.

Hung, W. C., F. Y. Chen, and H. W. Huang. 2000. Order-disorder transition in bilayers of diphytanoylphosphatidylcholine. *Biochim. Biophys. Acta.* 1467:198–206.

Huster, D., A. J. Jin, K. Arnold, and K. Gawrisch. 1997. Water permeability of polyunsaturated lipid membranes measured by ^{17}O NMR. *Biophys. J.* 73:855–864.

Huster, D., G. Paasche, U. Dietrich, O. Zschörnig, T. Gutberlet, K. Gawrisch, and K. Arnold. 1999. Investigation of phospholipid area compression induced by calcium-mediated dextran sulfate interaction. *Biophys. J.* 77:879–887.

Ichimori, H., T. Hata, H. Matsuki, and S. Kaneshima. 1998. Barotropic phase transitions and pressure-induced interdigitation on bilayer membranes of phospholipids with varying acyl chain lengths. *Biochim. Biophys. Acta.* 1414:165–174.

Jandacek, R. J., and W. B. Broering. 1989. X-ray diffraction study of sodium soaps of monounsaturated and polyunsaturated fatty acids. *Lipids.* 24:1008–1013.

Janiak, M. J., D. M. Small, and G. G. Shipley. 1979. Temperature and compositional dependence of the structure of hydrated dimyristoyl lecithin. *J. Biol. Chem.* 254:6068–6078.

Jürgens, E., G. Höhne, and E. Sackmann. 1983. Calorimetric study of the dipalmitoylphosphatidylcholine/water phase diagram. *Ber. Bunsengesells. Phys. Chem.* 87:95–104.

Kim, J. T., J. Mattai, and G. G. Shipley. 1987. Gel phase polymorphism in ether-linked dihexadecylphosphatidylcholine bilayers. *Biochemistry.* 26: 6592–6598.

Kodati, V. R., and M. Lafleur. 1993. Comparison between orientational and conformational orders in fluid bilayers. *Biophys. J.* 64:163–170.

Koenig, B. W., H. H. Strey, and K. Gawrisch. 1997. Membrane lateral compressibility measured by NMR and x-ray diffraction. *Biophys. J.* 73:1954–1966.

Koynova, R., and M. Caffrey. 1998. Phases and phase transitions of phosphatidylcholines. *Biochim. Biophys. Acta.* 1376:91–145.

Lafleur, M., B. Fine, E. Sternin, P. R. Cullis, and M. Bloom. 1989. Smoothed orientational order profile of lipid bilayers by ^{2}H NMR. *Biophys. J.* 56:1037–1041.

Le Bihan, T., and M. Pezolet. 1998. Study of the structure and phase behavior of dipalmitoylphosphatidylcholine by infrared spectroscopy: characterization of the pretransition and subtransition. *Chem. Phys. Lipids.* 94:13–33.

Litman, B. J., E. N. Lewis, and I. W. Levin. 1991. Packing characteristics of highly unsaturated bilayer lipids: Raman spectroscopic studies of multilamellar phosphatidylcholine dispersions. *Biochemistry.* 30: 313–319.

Luzzati, V. 1968. X-Ray Diffraction Studies of Lipid-Water Systems. Academic Press, London.

McCabe, M. A., and S. R. Wassall. 1995. Fast-Fourier-transform dePakeing. *J. Magn. Res. B.* 106:80–82.

Mitchell, D. C., K. Gawrisch, B. J. Litman, and N. Salem, Jr. 1998. Why is docosahexaenoic acid essential for nervous system function? *Biochem. Soc. Trans.* 26:365–370.

Nagle, J. F., and S. Tristam-Nagle. 2000. Structure of lipid bilayers. *Biochim. Biophys. Acta.* 1469:159–195.

Olbrich, K., W. Rawicz, D. Needham, and E. Evans. 2000. Water permeability and mechanical strength of polyunsaturated lipid bilayers. *Biophys. J.* 79:321–327.

Paddy, M. R., F. W. Dahlquist, E. A. Dratz, and A. J. Deese. 1985. Simultaneous observation of order and dynamics at several defined positions in single acyl chain using ^{2}H NMR of single acyl chain perdeuterated phosphatidylcholines. *Biochemistry.* 24:5988–5995.

Parsegian, V. A., N. Fuller, and R. P. Rand. 1979. Measured work of deformation and repulsion of lecithin bilayers. *Proc. Natl. Acad. Sci. U.S.A.* 76:2750–2754.

Pascher, I., M. Lundmark, P.-G. Nyholm, and S. Sundell. 1992. Crystal structures of membrane lipids. *Biochim. Biophys. Acta.* 1113:339–373.

Pohle, W., C. Selle, H. Fritzsche, and H. Binder. 1998. Fourier transform infrared spectroscopy as a probe for the study of the hydration of lipid self-assemblies. I. Methodology and general phenomena. *Biospectroscopy.* 4:267–280.

Rand, R. P., and V. A. Parsegian. 1989. Hydration forces between phospholipid bilayers. *Biochim. Biophys. Acta.* 988:351–376.

Rawicz, W., K. C. Olbrich, T. McIntosh, D. Needham, and E. Evans. 2000. Effect of chain length and unsaturation on elasticity of lipid bilayers. *Biophys. J.* 79:328–339.

Salmon, A., S. W. Dodd, G. D. Williams, J. M. Beach, and M. F. Brown. 1987. Configurational statistics of acyl chains in polyunsaturated lipid bilayers from ^{2}H NMR. *J. Am. Chem. Soc.* 109:2600–2609.

Schiller, J., J. Arnhold, S. Bernard, M. Müller, S. Reichl, and K. Arnold. 1998. Lipid analysis by matrix-assisted laser desorption and ionization mass spectrometry: a methodological approach. *Anal. Biochem.* 267: 46–56.

Separovic, F., and K. Gawrisch. 1996. Effect of unsaturation on the chain order of phosphatidylcholines in a dioleylphosphatidylethanolamine matrix. *Biophys. J.* 71:274–282.

Sternin, E., M. Bloom, and A. L. Mackey. 1983. De-Pakeing of NMR spectra. *J. Magn. Res.* 55:274–282.

White, D. A. 1973. Phospholipid Composition of Mammalian Tissues. Elsevier Scientific, New York.